Local Targeting of Malignant Gliomas by the Diffusible Peptidic Vector 1,4,7,10-Tetraazacyclododecane-1-Glutaric Acid-4,7,10-Triacetic Acid-Substance P

Stefan Kneifel,[1] Dominik Cordier,[3] Stephan Good,[2] Mihai C.S. Ionescu,[4] Anthony Ghaffari,[3] Silvia Hofer,[3] Martin Kretzschmar,[5] Markus Tolnay,[6] Christos Apostolidis,[7] Beatrice Waser,[8] Marlene Arnold,[8] Jan Mueller-Brand,[1] Helmut R. Maecke,[1,2] Jean Claude Reubi,[8] and Adrian Merlo[3,4]

Abstract

Purpose: Malignant glial brain tumors consistently overexpress neurokinin type 1 receptors. In classic seed-based brachytherapy, one to several rigid ^{125}I seeds are inserted, mainly for the treatment of small low-grade gliomas. The complex geometry of rapidly proliferating high-grade gliomas requires a diffusible system targeting tumor-associated surface structures to saturate the tumor, including its margins.

Experimental Design: We developed a new targeting vector by conjugating the chelator 1,4,7,10-tetraazacyclododecane-1-glutaric acid-4,7,10-triacetic acid to Arg^1 of substance P, generating a radiopharmaceutical with a molecular weight of 1,806 Da and an IC_{50} of 0.88 $\pm$ 0.34 nmol/L. Cell biological studies were done with glioblastoma cell lines. neurokinin type-1 receptor (NK1R) autoradiography was done with 58 tumor biopsies. For labeling, ^{90}Y was mostly used. To reduce the "cross-fire effect" in critically located tumors, ^{177}Lut and ^{213}Bi were used instead. In a pilot study, we assessed feasibility, biodistribution, and early and long-term toxicity following i.t. injection of radiolabeled 1,4,7,10-tetraazacyclododecane-1-glutaric acid-4,7,10-triacetic acid substance P in 14 glioblastoma and six glioma patients of WHO grades 2 to 3.

Results: Autoradiography disclosed overexpression of NK1R in 55 of 58 gliomas of WHO grades 2 to 4. Internalization of the peptidic vector was found to be specific. Clinically, the radiopharmeutical was distributed according to tumor geometry. Only transient toxicity was seen as symptomatic radiogenic edema in one patient (observation period, 7-66 months). Disease stabilization and/or improved neurologic status was observed in 13 of 20 patients. Secondary resection disclosed widespread radiation necrosis with improved demarcation.

Conclusions: Targeted radiotherapy using diffusible peptidic vectors represents an innovative strategy for local control of malignant gliomas, which will be further assessed as a neoadjuvant approach.

Authors' Affiliations: [1]Clinic and Institute of Nuclear Medicine, [2]Division of Radiological Chemistry, [3]Neurosurgical Clinic, [4]Molecular Neuro-Oncology Laboratory of the Department of Surgery and Research, [5]Neuroradiology, and [6]Neuropathology, University Hospitals, Basel, Switzerland; [7]European Commission, Joint Research Centre, Institute for Transuranium Elements, Karlsruhe, Germany; and [8]Division of Cell Biology and Experimental Cancer Research, Institute of Pathology, University of Berne, Berne, Switzerland

Received 12/27/05; revised 3/29/06; accepted 4/7/06.

Grant support: Swiss National Science Foundation Tandem grants 3238-056368.99/1 and 3238-069472/2.

The costs of publication of this article were defrayed in part by the payment of page charges. This article must therefore be hereby marked *advertisement* in accordance with 18 U.S.C. Section 1734 solely to indicate this fact.

Note: Supplementary data for this article are available at Clinical Cancer Research Online (http://clincancerres.aacrjournals.org/).

S. Kneifel and D. Cordier contributed equally to this work.

Requests for reprints: Adrian Merlo, Neurosurgical Clinic, University Hospital Basel, Spitalstrasse 21, 4031 Basel, Switzerland. Phone: 41-61-265-71-82; Fax: 41-61-265-71-38; E-mail: amerlo@uhbs.ch.

doi:10.1158/1078-0432.CCR-05-2820

Histologic differentiation, the degree of tumor cell infiltration into adjacent normal brain tissue and variable growth rates (1–3), determines mean survival in primary malignant gliomas, which varies between nearly 10 years in low-grade oligodendroglioma WHO II (4) and 10 to 14 months in highly proliferative glioblastoma (5, 6). Survival differences and response to therapy are regulated by genetic factors (7). Despite technological advances in diagnosis and treatment, prognosis of malignant gliomas remains unchanged (8). With regard to low-grade gliomas that affect a younger age group, there is considerable variability in diagnostic criteria over time (9) and in deciding when and how to initiate treatment. The fact that brain-intrinsic neoplasms represent the second most frequent cancer-related cause of death in adolescents and younger adults between the age of 15 and 35 after leukemias (10) underscores the need for innovative treatment strategies.

Because 95% of glioblastomas manifest as unifocal lesion that recur within a 2-cm margin at the primary site (11),

loco-regional drug application has become a therapeutic option, using bifunctional molecules that consist of a targeting domain [e.g., the transferrin receptor (12), the interleukin-4 and interleukin-13 receptors (13, 14), or a monoclonal antibody against tenascin-C (15–17)] and of an effector domain [e.g., bacterial toxins (12–14) or radioisotopes (18)]. Toxin-delivering conjugates have to target every single tumor cell; radionuclide-based approaches can eliminate receptor-negative tumor cells and cells not directly targeted by the drug through the range-dependent "cross-fire" effect. Most protocols for targeted local therapy of malignant brain tumors administer macromolecular compounds given by convection-enhanced delivery to improve biodistribution (13). Labeling vectors with short-lived radioisotopes [e.g., the α-emitter ^{213}Bi ($t_{1/2}$ = 46 minutes)], however, require rapid i.t. diffusion only achievable with small drug-like sized vectors. The prototypical low molecular weight (1.3 kDa) vector [^{90}Y/^{111}In-DOTA^{0}D-Phe^1-Tyr^3]-octreotide targets somatostatin type 2 receptor (SSTR2)–positive tumors [e.g., neuroendocrine tumors (19, 20), relapsing medulloblastoma (21), and SSTR2-positive gliomas (22)]. However, inconsistent expression of SSTR2 limited application in glioblastoma. We, therefore, developed a new bifunctional peptidic vector that targets the neurokinin type-1 receptor (NK1R), which is consistently overexpressed in primary malignant gliomas (23). Its major ligand substance P (SP) belongs to the family of tachykinin peptide neurotransmitters (24). Besides physiologic expression on distinct interneuron populations of the afferent spinal pain and the limbic system, NK1 receptors have been detected only at restricted sites within the central nervous system (e.g., on reactive mammalian astrocytes in lesions of multiple sclerosis; ref. 25). We conjugated the chelator 1,4,7,10-tetraazacyclododecane-1-glutaric acid-4,7,10-triacetic acid (DOTAGA; ref. 18) to Arg^1 of the linear 11-mer peptide SP, generating a radiopharmaceutical with a molecular weight of 1,806 Da (DOTAGA-Arg^1-SP). Following preclinical assessment, we conducted a pilot study in 20 patients with gliomas of WHO grades 2 to 4 to primarily assess biodistribution and short-term and long-term toxicity and to assess as secondary end points the clinical and radiological responses.

Materials and Methods

Human glioma cells LN319 (26, 27) were grown to a confluence of 80% to 90% in standard conditions (28). Oregon Green 488 fluorescent SP (SP-OG, Invitrogen AG, Basel, Switzerland) was used at 100 nmol/L for the time course studies. Concentration dependence was determined after 6 hours of incubation. Unlabeled SP (10 μmol/L) was added for competitive blocking of the receptor-mediated uptake of SP-OG. Transfections and flow cytometry studies have been done to assess ligand internalization and the effect on cell cycle and apoptosis. SP receptor was overexpressed in LN319 cells, using the DNA fragment that encodes the long splice variant of the human receptor (Genbank accession no. NM_001058). PCR amplification was carried out using Pfu DNA Polymerase (Promega, Madison, WI) and primers with an *Eco*RI restriction site at the 5′ and an *Xho*I site at the 3′ end (5′_NK1R_*Eco*RI, 5′-GTGCGGAATTCGCCACCATGGATAACGTCCTCC; 3′_NK1R_*Xho*I, 5′-GAACCGCTCGAGGGAGAGCACATTGGAGGAGAA). The PCR product was cloned into the pcDNA3 eukaryotic expression vector (Invitrogen). Fixed cells were analyzed with a FACScan flow cytometer and CellQuest software (Becton Dickinson, Franklin Lakes, NJ), counting at least 50,000 events. Cell cycle and apoptosis were investigated using propidium iodide and Annexin V-FITC (BD Biosciences, Allschwil, Switzerland), respectively. Propidium iodide was used at 10 μg/mL.

Receptor autoradiography. Surgical specimens consisting of 34 glioblastomas, 9 oligodendrogliomas II/III, and 15 astrocytomas II/III were obtained after surgical resection and processed as described (23, 29). Receptor density was quantified using ^{125}I-Bolton-Hunter-SP and a cutoff of at least twice the value estimated for the nonspecific binding (29, 30). The IC_{50} value for Lu-DOTAGA-SP at the NK1R was determined in competition experiments with successive tumor tissue sections.

Radioconjugates. Chemical synthesis of the radiopharmaceutical is described. The peptides were assembled on solid phase with a semiautomatic peptide synthesizer (RinkCombichem Technologies, Bubendorf, Switzerland) using fluorenylmethoxy-carbonylpolyamide solid-phase peptide synthesis (31). DOTAGA(^{t}Bu)$_4$-OH was introduced as a protected prochelator at the NH_2-terminal of the undecapeptide (32). After deprotection and purification using RP-HPLC (Bischoff HPLC system, Metrohm AG, Herisau, Switzerland), the chelator peptide conjugate DOTAGA-SP was obtained in high purity [>95% high-performance liquid chromatography (HPLC)]. Identity was confirmed by matrix-assisted laser desorption/ionization-time of flight mass spectroscopy (Voyager-DE STR, Applied Biosystems, Framingham, MA). The chelator peptide conjugate was labeled with specific activity of 67.3 MBq/nmol for ^{90}Y (Perkin-Elmer, Billerica, MA), of 67.3 MBq/nmol for ^{177}Lu (IDB, Petten, the Netherlands), and of 11 MBq/nmol for ^{213}Bi (^{225}Ac/^{213}Bi generator, ITU, Karlsruhe, Germany) for therapy. For diagnosis, 2 MBq of ^{111}In (Mallinckrodt Med, Petten, the Netherlands) were used. These radionuclides exhibit the following physical properties: $^{90}YCl_3$ (maximum β^- energy = 2.27 MeV, $t_{1/2}$ = 64 hours, maximum range = 12 mm), $^{177}LuCl_3$ (maximum β^- energy = 0.5 MeV, $t_{1/2}$ 161 hours, maximum range = 1.5 mm), $^{213}BiCl_3$ (maximum α-energy = 5.98 MeV, $t_{1/2}$ 46 = minutes, maximum range = 0.06 mm), and $^{111}InCl_3$ (energy = 247 keV, $t_{1/2}$ = 67.9 hours). The conjugate was dissolved in 500 μL sterile filtered buffer containing 16.4 mg sodium acetate, 18.5 mg 2,5-dihydroxybenzoic acid, and 0.1 g of L(+)-ascorbic acid sodium salt. The radiometal was added and incubated for 30 minutes at 95°C. Quality control was done using RP-HPLC (Macherey-Nagel CC 250/4 Nucleosil 120-3 C18, flow = 0.75 mL/min; eluents: A = acetonitrile, B = 0.1% trifluoroacetic acid in water; gradient: 0 minutes, 95% B; 30 minutes, 55% B; 32 minutes, 0% B; 34 minutes, 0% B; 37 minutes, 95% B; retention time = 23 minutes). A radiochemical purity of >99% was achieved for ^{90}Y and ^{177}Lu and >90% for ^{111}In. ^{213}Bi was eluted from a ^{225}Ac/^{213}Bi generator provided by the Institut for Transuranium Elements, with 2.0 mol/L HCl (33). Labeling with ^{213}Bi required an additional cleaning step using a Sep-Pak C18 cartridge (Waters, Milford, MA). The solution was immobilized on the cartridge, washed with 10 mL of a 0.4 mol/L sodium acetate buffer (pH 5), and eluted with 10 mL methanol. After evaporation, a radiochemical purity of about 90% was achieved. For injection, the solution was diluted to a volume of 1 mL with 0.9% NaCl.

Patients. The clinical data of the 20 patients enrolled into the study are shown in Table 1. The protocol had been approved by the Ethical Committee of the University Hospitals of Basel. Response criteria as proposed by Macdonald were applied (34). Patients with high-grade lesions (n = 16) were included following progression or denial of conventional treatment options. The four low-grade glioma patients selected targeted radiotherapy instead of an observational phase or external beam radiotherapy. Patients were evaluated weekly for the first month and thereafter according to the course of the disease. Functional status was assessed using the Barthel index.

Injection of the radiopharmaceutical. In all cases, injection of the drug has been done via an implanted catheter system (16, 22, 35), either into the tumor or into the resection cavity. The catheter itself is connected to a s.c. port, which is punctured for the injection of the drug. Preparation of the patient with 20 mg dexamethasone and, immediately before injection, 60 g of the osmodiuretic drug mannitol

Table 1. Clinical data of patients treated with targeted radiotherapy using DOTAGA-SP

No.	Age/ gender	Histology/ location	Treatment before/after targeted RT	Total activity (MBq)/ radionuclide	Barthel index before/at the end of targeted RT	Survival after initiation of targeted RT	Overall survival*
Glioblastomas							
19-1	37/F	G/fL	S-R-C	375/^{213}Bi	80/70	7	26
8-2	52/M	G/ftR	S-C/−	5250/^{90}Y	100/95	24	25
2-3	60/F	G/pL	R-S/S	5250/^{90}Y	95/95	18	23
16-4	21/F	G/pons	*R-C/−	1125/^{177}Lut	15/70	10	20
6-5	66/F	G/pL	S/C	3750/^{90}Y	100/90	18	19
12-6	57/F	G/poL	*S/−	5625/^{90}Y	95/90	18	19
7-7	47/F	G/fpR	S-R-C/S	4500/^{90}Y	5/40	9	17
1-8	69/M	G/tR	S/−	4688/^{90}Y	90/90	15	16
13-9	50/M	G/bifcR	S-C-R	1875/^{90}Y	25/35	8	15
4-10	40/M	G/fR	S/−	7500/^{90}Y	100/95	13	14
5-11	63/M	G/ ftR	S-R-C/−	5250/^{90}Y	30/50	11	14
14-12	44/F	G/thL	*−/−	4875/^{90}Y	15/65	8	9
15-13	71/F	G/tpL	*−/−	3750/^{90}Y	100/65	6	7
3-14	70/M	G/fL	S/−	7500/^{90}Y	100/75	6	7
Gliomas WHO grades 2-3							
17-15	37/F	OAIII/thR	S-C/−	2250/^{177}Lut	40/75	+20	+149
20-16	42/M	OII/pcL	S/S	825/^{213}Bi	90/90	+66	+67
10-17	34/M	AII/pfL	S/S	7500/^{90}Y	100/100	+26	+41
9-18	63/M	AIII/toL	*R-C/S	6375/^{177}Lut	60/95	11	28
11-19	34/M	OII/fR	*−/S	5625/^{90}Y	100/100	+28	+29
18-20	31/M	OII/fL	*−/S	2250/^{90}Y	100/100	+22	+23

Abbreviations: G, glioblastoma multiforme; A, astrocytoma; OA, oligoastrocytoma; O, oligodendroglioma; I-IV, WHO grade 1-4; f, frontal; t, temporal; p, parietal; o, occipital; th, thalamic; L, left; R, right; S, surgery; RT, radiotherapy; R, external beam radiotherapy; C, chemotherapy.
*+: alive; *, i.t. injection, no surgery before targeted radiotherapy.

leads to a transient and very efficient reduction of the i.t. pressure that allows to inject the radiopharmaceutical against low resistance as previously described (22). Before injection of the active compound, the system is flushed with 1.5 mL of human albumin 5% over 1 minute to coat the plastic surface. Thereafter, the active drug is injected in a volume of 2 mL over 1 minute. Finally, the system is flushed again with 1.5 mL of human albumin 5% over 1 minute.

Positron emission tomography, single photon emission-tomography, and perfusion computed tomography. Positron emission tomography was done following standard protocols after application of [^{18}F]fluorodeoxyglucose. For anatomic correlation of single-photon emission computed tomography (SPECT) with CT scans, patients were coinjected with 500 MBq [^{99m}Tc]Neurolite (Bristol-Myers Squibb, Billerica, MA) as a marker for brain perfusion. Three SPECT scans were done after each administration of the radiopharmaceutical; scan duration was 30 minutes with continuous acquisition on a dual-head camera (Picker P2000, Philips Medical Systems, Eindhoven, the Netherlands). Scans were acquired with a medium-energy collimator in multiple energy windows to distinguish between ^{99m}Tc and ^{111}In or ^{90}Y [Pretherapeutic dosimetry with ^{111}In: 140 keV (±7.5%) for ^{99m}Tc, 171 keV (±10%) and 245 keV (±10%) for ^{111}In. Therapeutic dosimetry: 140 keV (±7.5%) for ^{99m}Tc and 306 keV (±45%) for ^{90}Y bremsstrahlung]. Perfusion CT was done with a Somatrom Sensation 16 CT (Siemens Medical, Erlangen, Germany) following the recommended protocol of Siemens Medical. CBV and permeability values were calculated with the Syngo Perfusion software.

Stability and biodistribution of DOTAGA-Arg^1-SP. For all patients except for cases 9, 10, 11, and 18, planar scintigraphic images were obtained with a large field-of-view camera (DIACAM; Siemens Medical) as described (22, 35). In these cases, tumor dosimetry was estimated according to the published protocol (22). Due to large error ranges of at least ±20% (22), we developed a novel approach to measure the tumor dose that allows an individual three-dimensional voxelwise dosimetry by fusing therapeutic SPECT images with the tumor images[9] as shown for patients 9, 10, 11, and 18. In this trial, dosimetry data could only be calculated for cases 10 and 18 using this new protocol. Following pretherapeutic dosimetry with 2 MBq [^{111}In]-DOTAGA-SP, therapeutic dosimetry was done after application of 370 to 3,330 MBq [^{90}Y]-DOTAGA-SP. After iterative reconstruction of the three SPECT images following injection of the radiopharmaceutical, filtering with a low-pass filter and correction for attenuation coefficients, fusion of SPECT and CT scan was done manually (Fusion software: MPI-Tool, Advanced Tomo Vision, Kerpen, Germany). Outlines of the [^{99m}Tc]-ECD image were projected onto a spatially corrected contrast-enhanced CT scan before matching with the coacquired ^{111}In or ^{90}Y images. Assuming an average energy deposition of 930.8 keV per ^{90}Y β decay and a density of 1.0 g/cm^3 of the absorbing tissue, quantitative dose distribution maps in Gray could be mathematically calculated.

The chemical integrity of the radioligand in blood, cerebrospinal fluid, and resection cavity fluid was examined as described. HPLC (Bischoff HPLC System, Metrohm AG, Herisau, Switzerland) and a radioactivity detector (LB509 Radioflow Detector, Berthold Technologies GmbH, Regensdorf, Switzerland) were used. Stabilities were tested using radiolabeled substance in a concentration of 1.8 μmol/L in 500 μL cerebrospinal fluid and 100 μL 0.1 mol/L Ca-diethylenetriaminepentaacetic acid at 37°C. After incubation, aliquots of 100 μL were

[9] In preparation.

mixed with 200 μL ethanol to precipitate proteins. After centrifugation, the clear supernatants were analyzed by HPLC (Macherey-Nagel CC 250/4 Nucleosil 120-3 C18, flow: 0.75 mL/min; eluents: A = acetonitrile, B = 0.1% trifluoroacetic acid in water; gradient: 0 minutes, 95% B; 30 minutes, 55% B; 32 minutes, 0% B; 34 minutes, 0% B; 37 minutes, 95% B). Stability of the metal-chelator complex was tested using DOTAGA-D-Phe-NH_2 as a model for the biomolecule-bound chelator. The radiolabeled compound was incubated at 37°C and pH 5 (0.4 mol/L sodium acetate buffer) with 10^4 fold excess of Ca-diethylenetriaminepentaacetic acid to trap decomplexed metal. Over a period of 10 days, samples of this solution were analyzed by HPLC using a radioactivity detector for quantification of the decomplexation.

Results

Incidence of NK1R and binding affinity of DOTAGA-SP. Thirty-two of 34 glioblastomas (94%), 7 of 9 oligodendrogliomas II/III, and 15 of 15 astrocytomas overexpressed NK1R (Fig. 1A), with mean densities of 4,593 ± 798, 8,324 ± 1,950, and 5,044 ± 1,428 dpm/mg tissue in autoradiography. NK1-, NK2-, and NK3-selective ligands allowed classification of the SP-binding sites as NK1R (Fig. 1A). Background radioactivity was below 5%. Typical displacement of bound ^{125}I-Bolton-Hunter-SP by low concentrations of SP, but not by the NK2R-selective [Nle^{10}]-neurokinin A(4-10) or the NK3R-selective ligand, indicated specific localization of NK1R in glial tumors. The IC_{50} values for ^{177}Lu-DOTAGA-SP and ^{90}Y-DOTATA-SP were 0.88 ± 0.34 and 1.0 ± 0.37 nmol/L, respectively, as assessed by autoradiography in competition experiments (ref. 29; Fig. 1B).

Receptor-mediated uptake of SP conjugates. Flow cytometric analysis revealed bright staining of LN319 glioblastoma cells following incubation with 100 nmol/L SP-OG (EC_{50} = 30 nmol/L). Coincubation with 10 μmol/L of unlabeled SP resulted in a 90% block of SP-OG internalization (Fig. 1C). Overexpression of NK1R full-length cDNA in LN319 glioblastoma cells by transient transfection accelerated the kinetics of SP-OG internalization compared with nontransfected cells, not

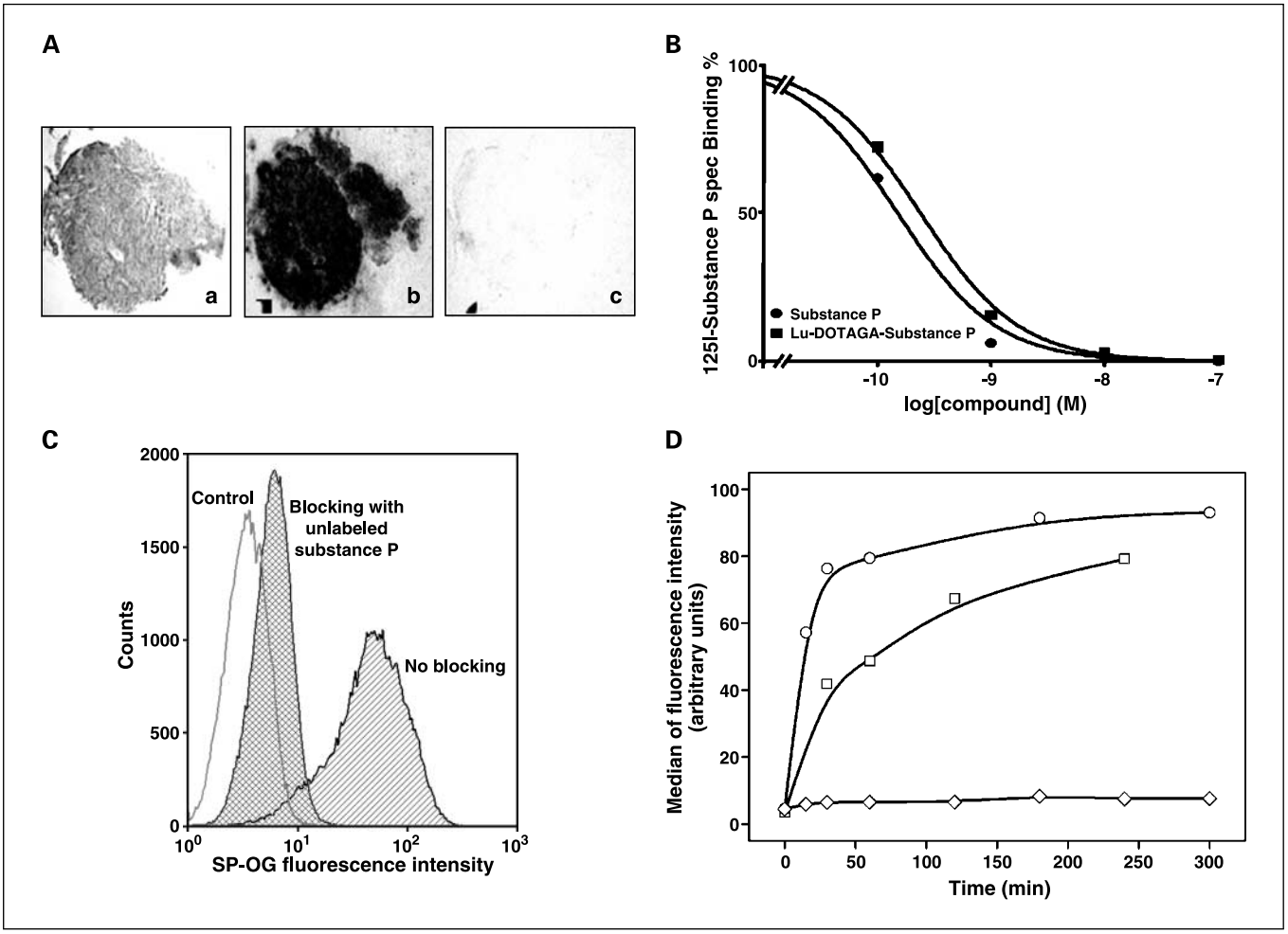

Fig. 1. NK-1 expression and specific receptor-mediated uptake of SP in malignant gliomas. *A,* autoradiography shows high and homogenous expression of NK1R in a representative glioblastoma as described (22, 46): *a,* H&E staining; *b,* autoradiogram showing total binding of ^{125}I-Bolton-Hunter-SP (black labeling shows NK1R expression in tumor); *c,* autoradiogram (in the presence of excess cold peptide). *B,* competition experiment in successive sections of a glioblastoma with ^{125}I-Bolton Hunter-SP showing complete and high-affinity displacement of ^{177}Lu-DOTAGA-SP (■) and of the control peptide SP (●). *C,* flow cytometry analysis of LN319 cells incubated with 100 nmol/L SP-OR shows specific uptake of the ligand, which can be blocked with 10 μmol/L SP. Control histogram shows cells not exposed to SP-OG. *D,* time course of the SP-OG internalization by LN319 cells. Cells transiently transfected with the NK1R pcDNA3 eukaryotic expression vector (○), untransfected cells (□), blocking of internalization with unlabeled SP (◇).

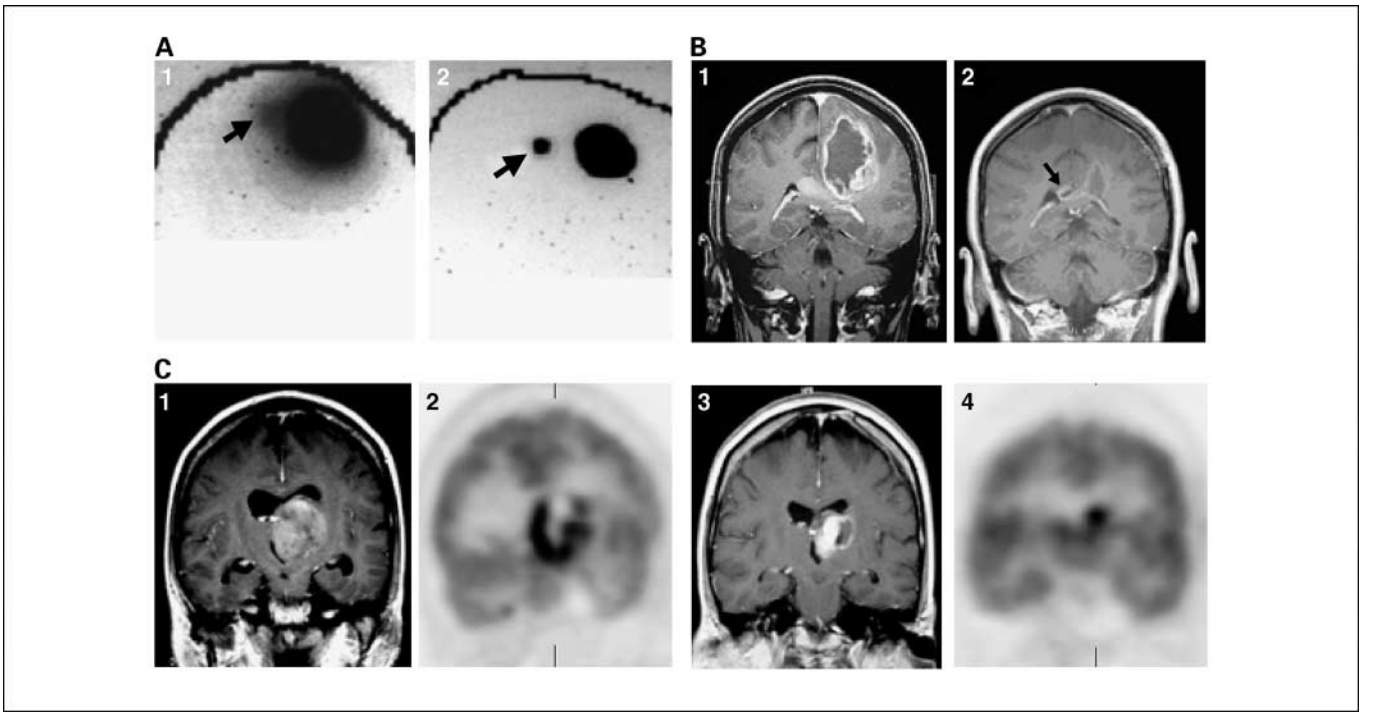

Fig. 2. Radiologic response in deep-seated glioblastoma. *A,* lateral planar scintigraphy 30 minutes (*1*) and 240 minutes (*2*) following i.t. injection of [^{111}In]-DOTAGA-SP marks glioblastoma satellite lesion (*arrow*). *B,* coronal planes of T_1-weighed magnetic resonance images with the contrast-agent gadolinium-DOTA show a large left-sided parieto-callosal glioblastoma (*1*) before and (*2*) 9 months after debulking surgery and targeted i.t. and intracavitary β-radiotherapy. Residual tumor at the resection margins and within the splenium of the corpus callosum (*arrow*) was efficiently controlled for 11 months (case 6; Table 1). *C,* coronal planes of T_1-weighed magnetic resonance images with the contrast-agent gadolinium-DOTA (*1* and *3*) and [^{18}F]-deoxyglucose PET images (*2* and *4*) show an inoperable large glioblastoma in the left thalamus (case 12, Table 1). A partial response (*3* and *4*) was observed 3 months after targeted i.t. β-radiotherapy using [^{90}Y]-DOTAGA-SP, leading to clinical improvement (15-65 points in Barthel index).

affecting the plateau saturation value (Fig. 1D). Incubation of LN319 glioblastoma cells with 30 nmol/L SP and with 10 nmol/L of ^{111}In-DOTAGA-SP (24 hours, 37°C) at 5- to 10-fold higher concentrations than the respective IC_{50} values did not affect cell cycle and cell survival (data not shown).

Pharmacokinetics of radiolabeled DOTAGA-SP. DOTAGA permits stable labeling with $^{90}YCl_3$, $^{177}LuCl_3$, and $^{213}BiCl$. Incubation at 37°C with 10^4-fold excess of Ca-diethylenetriaminepentaacetic acid to trap decomplexed metal resulted in <2% release of radiometal after 300 hours (36). Metabolic stability of DOTAGA-SP was dependent upon the degree of contamination of cerebrospinal fluid with serum. *In vitro* incubation of [^{90}Y]-DOTAGA-SP in serum-free cerebrospinal fluid obtained from control patients exhibited a stability of 84% after 24 hours. In serum-contaminated cerebrospinal fluid, complete metabolic degradation was observed within 30 hours, displaying the same HPLC peaks as seen in 24-hour urine samples of patients after injection of [^{90}Y]-DOTAGA-SP. Serum residence time of [^{90}Y]-DOTAGA-SP is only 1 to 2 minutes due to rapid degradation and renal clearance, distinct from tubular reuptake as known for octreotide-based peptidic vectors (22). Twenty-four-hour urine samples showed that 60% to 70% of the locally injected radioactivity had been excreted. The remaining activity was confined to the target site as shown on whole body scans. Only in the urinary bladder and in the kidneys, faint signals were obtained in whole-body scintigrams, which were slightly above background radioactivity levels. All other organs were negative on whole-body scintigrams during the 72 hours of observation period. Diffusibility of [^{111}In]-DOTAGA-SP is shown by marking a glioblastoma satellite lesion 4 hours following i.t. injection (Fig. 2A).

DOTAGA-SP in glioblastomas. In 14 glioblastoma, local injections of radiolabeled DOTAGA-SP were done (Table 1). Except for the glioblastoma in case 2 that grew out of an astrocytoma grade 2, all grade 4 tumors were primary glioblastomas. The first patient (case 8) received 4,687.5 MBq of [^{90}Y]-DOTAGA-SP in eight fractions into the resection cavity following tumor debulking as only additional treatment, leading to a survival time of 16 months. In the second treated patient (case 6), the resection rim and residual callosal tumor spread were targeted by intracavitary (3,000 MBq) and i.t. (2625 MBq) administration of [^{90}Y]-DOTAGA-SP as only treatment after surgery, resulting in (*a*) objective radiological response of the callosal tumor nodule and (*b*) recurrence-free survival time of 11 and overall survival time of 19 months (Fig. 2A). Absence of drug-related toxicity and objective responses encouraged expansion of this approach to another 12 glioblastoma patients. Impaired neurologic function improved in 5 of 14 glioblastoma patients (cases 4, 7, 9, 11, and 12) within 2 weeks after initiation of targeted radiotherapy (Table 1), a phenomenon not detectable during external beam radiotherapy. In cases 4, 6 (callosal nodule, see above), 12, and 13, radiolabeled DOTAGA-SP was directly injected into the nodular tumor without previous surgery, which allowed to directly assess the effects on the targeted tumor. Two such cases are highlighted (cases 4 and 12). In case 12, a large left-sided thalamic glioblastoma in a 45-year-old woman with increased i.c. pressure, right-sided hemiparesis, and aphasia was only

treated with this new modality with a cumulative activity of 4,810 MBq [^{90}Y]-DOTAGA-SP, leading to marked clinical improvement (15-65, Barthel index) and a partial radiologic response (Fig. 2B). In case 4 pretreated with external beam radiotherapy (54 Gy) and temozolomide chemotherapy, 1,125 MBq [^{177}Lu]-DOTAGA-SP were injected into a progressive pontine glioblastoma via a transcerebellar catheter without side effects. Clinical (15-70, Barthel index) and radiologic improvement lasted for 5 months. In cases 3 and 7, surgical debulking was done after targeted radiotherapy, which disclosed extensive radiation necrosis. As secondary end points, we assessed survival after initiation of targeted radiotherapy and overall survival (Table 1). In glioblastoma, median survival after initiation of this local treatment was 11 months (range, 6-24 months), and median overall survival was 16 months (range, 7-26 months).

DOTAGA-SP in malignant gliomas WHO grades 2 and 3. To assess intermediate and long-term toxicity, two anaplastic gliomas WHO grade 3 and four low-grade gliomas WHO grade 2 were included (Table 1). Impaired neurologic function markedly improved in two of these six patients (cases 15 and 18) within 2 weeks after the injection of the radiopharmaceutical (Table 1). Because of critical tumor location in case 18, the less energetic [^{177}Lu]-DOTAGA-SP was used. Except for the anaplastic astrocytoma patient (case 18) that died from tumor progression, the remaining five patients could be evaluated for signs and symptoms of intermediate or long-term toxicity. No toxicity was noticed within a median observation period of 26 months (range, 14-66 months). This is important because the peptidic vector DOTAGA-SP is diffusible, and low amounts of NK-1 receptors are expressed at restricted sites in the mammalian central nervous system. In cases 16 to 20, surgical resection was done following i.t. (cases 18, 19, and 20) and intracavitary (cases 16 and 17) administration, which disclosed widespread radiation necrosis. In case 19, the initially nonenhancing hypodense lesion demarcated as a perifocal ring-enhancing structure with central hypodensity and *de novo* peripheral calcification, suggestive for radiation necrosis according to perfusion CT imaging (Siemens software; Fig. 3D and E). Craniotomy became necessary 27 months following i.t. injection of DOTAGA-SP due to signs of i.c. pressure requiring steroid medication. Surgery was considerably facilitated due to improved demarcation of margins (Supplementary Video). Histologic work-up disclosed a calcified, completely radionecrotic lesion.

α-Emitter ^{213}Bi for labeling DOTAGA-SP. ^{90}Y has a maximum tissue range of 12 mm, potentially inducing collateral damage. Radionuclides dissipating their energy in the micrometer range are theoretically superior for the treatment of invasive tumor cells not visible beyond the radiological tumor

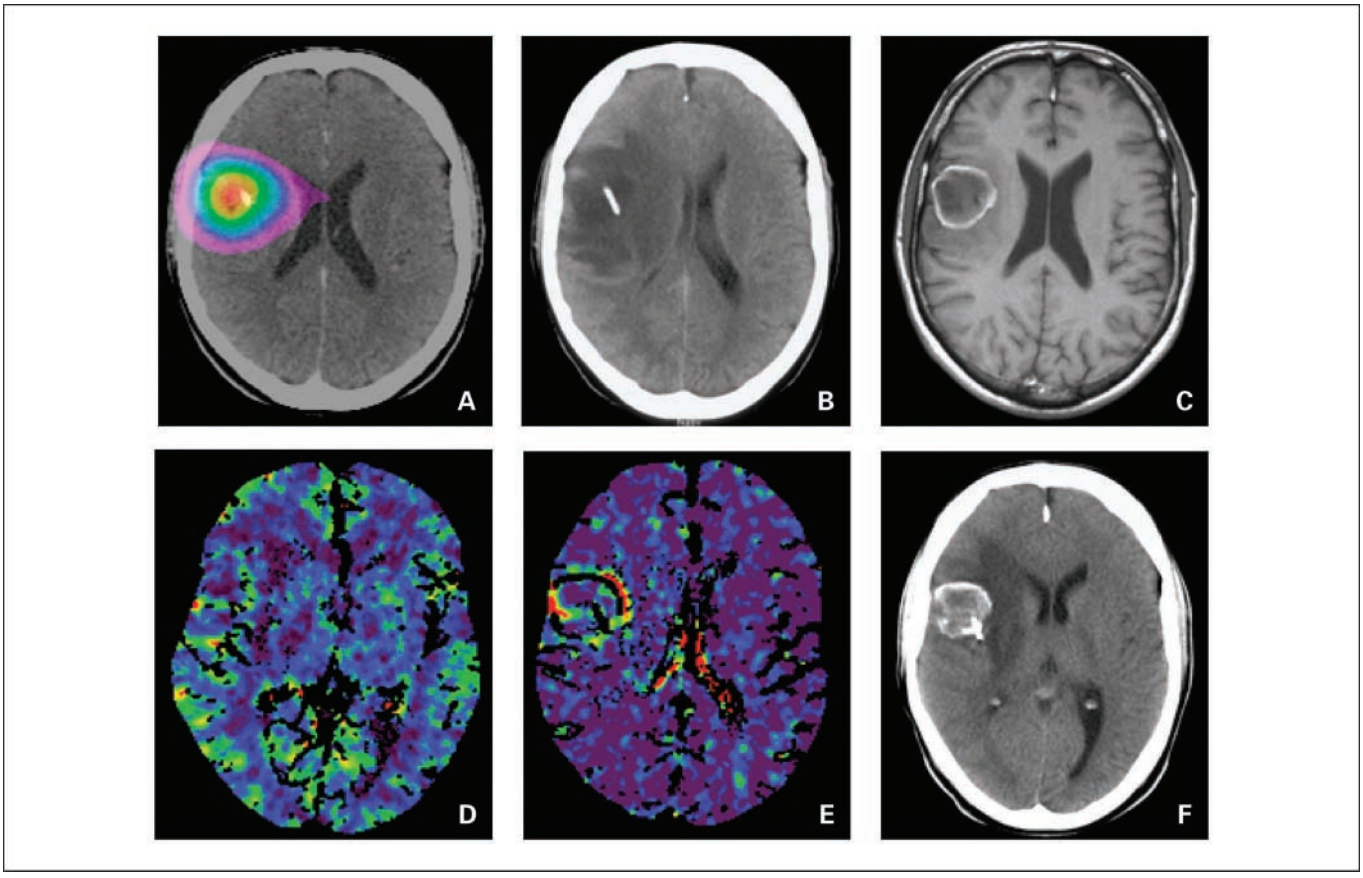

Fig. 3. CT-SPECT fusion imaging shows orthotopic distribution of [^{90}Y]-DOTAGA-SP. Axial planes of CT scans show a frontal oligodendroglioma WHO II on the right (case 19) directly after i.t. injection of 1,125 MBq [^{90}Y]-DOTAGA-SP (*A*) and 2 weeks later (*B*), displaying transient secondary perifocal edema reaction that is controlled with antiedematous therapy. Two years following treatment, perifocal calcification indicates radiation necrosis (*F*), according to perfusion CT imaging (Siemens software; *D* and *E*). Magnetic resonance imaging scans show a demarcated lesion as a perifocal ring-enhancing structure with central hypointensity (*C*).

margins. We, therefore, tested the feasibility of targeted radiotherapy with ^{213}Bi ($t_{1/2}$ = 46 minutes, maximum range = 0.06 mm) in a progressive glioblastoma (case 1) and in a postcentral low-grade oligodendroglioma WHO II (case 16). Intracavitary injection of 375 and of 825 MBq of [^{213}Bi]-DOTAGA-SP, respectively, was well tolerated. Response assessment was difficult in case 1 due to bulky residual tumor. In case 16, resection of a mass lesion 33 months after α-therapy had only disclosed radiation necrosis and absence of vital tumor cells. The further course had been excellent for another 34 months without any signs of tumor recurrence.

Dosimetry, functional outcome, and adverse events. Dosimetry based on fusion of CT/SPECT images had only become available for cases 17 and 20 in this study. In case 19, the cumulative absorbed energy per voxel was calculated to be 594 Gy following i.t. injection of 5,625 MBq of [^{90}Y]-DOTAGA-SP. In case 20, injection of 2,250 MBq of [^{90}Y]-DOTAGA-SP as two fractions resulted in 549 Gy. For the remaining cases, dose estimates had been done as previously reported (22). Values are not listed in Table 1 due to large error ranges. The functional status of the patients has been assessed using the Barthel index at initiation and 3 months after completion of targeted radiotherapy (37). Temporary improvement or stabilization was observed in 13 cases and gradual worsening in the remaining seven cases due to incomplete tumor control (Table 1). Transient perifocal edema reaction was controlled with corticosteroids. Secondary edema reaction was accompanied by a minor and transient paresis of the distal left arm in case 19 (Fig. 3B).

Discussion

The fact that 95% of malignant gliomas clinically manifest as unifocal lesions that also recur at the primary site (11) underscores the need for local therapies as one essential pillar of glioma treatment. Several bifunctional biomolecules, consisting of a targeting and an effector domain (12–17), have been developed. Intratumoral and/or intracavitary injection of the diffusible vector DOTAGA-SP represents a versatile new tool for the local control of malignant gliomas. Chelated peptides can be labeled with different radioisotopes with distinct chemico-physical properties. Saturation of the irregular structure of glioblastomas may best be achieved with a diffusible targeting system, as shown by marking a tumor satellite lesion (Fig. 2A). In addition, the "cross-fire" effect of β-emitting radionuclides allows to treat receptor-negative tumor cells and areas not sufficiently saturated by the drug. Conjugated SP showed high affinity to NK1R of brain tumor tissue, and the ligand showed specific uptake and internalization (Fig. 1). The prototypical octreotide-based vector [^{90}Y/^{111}In-DOTA^{0}D-Phe^{1}-Tyr^{3}]-octreotide (22, 35) had several drawbacks, which could be overcome by this new targeting system: (*a*) the cognate SP receptor NK1R is overexpressed in virtually all glial neoplasms, whereas expression of SSTR2 is low in most glioblastomas (29, 35, 38, 39); (*b*) NK1R expression in normal brain tissue is restricted to circumscribed areas, whereas SSTR2 are ubiquitously expressed, not allowing precise autoradiographic distinction between normal brain tissue and tumor cells in areas of tumor cell infiltration (35, 38); (*c*) strong expression of NK1R within the tumor neovasculature (23) suggests concomitant targeting of vascular structures; (*d*) labeling kinetics of the chelator DOTAGA (40) conjugated to SP are superior to DOTA (reaction rate, 10-fold higher) suitable for labeling with the α-particle emitter Bi-213; and finally, (*e*) first experience with DOTAGA-SP resulted in stronger clinical and radiologic responses compared with the prototypical sstr2 targeting system (22, 35). We have selected a peptidic vector that is stable at the target site for up to 72 hours but gets rapidly degraded within 1 to 2 minutes upon entry into systemic circulation due to serum peptidases. This minimizes the risk of systemic side effects from NK-1 expressing immune cells and from unspecific kidney problems due to tubular reuptake of the radiopharmaceutical (41). Unambiguous clinical and radiological responses were observed in cases of monotherapy with DOTAGA-SP, for instance, a partial response was seen in a large thalamic glioblastoma (case 9; Fig. 2B), accompanied by marked functional amelioration. Partial and lasting neurologic recovery was also seen in cases 4, 7, 11, 12, 15, and 18 following targeted radiotherapy. Case 4 represents a unique report of a locally treated progressive brainstem glioblastoma, which showed objective clinical and radiologic responses for 5 months. Thus far, only a few experimental reports have been published on brainstem gliomas in rodent models (42). Local therapies are generally used following tumor debulking to enhance tumor control at the resection rim (17, 43). In addition, i.t. application is also being investigated (44). The small drug-like vector DOTAGA-SP can either be injected into the resection cavity or directly into the tumor mass. In seven cases, DOTAGA-SP was directly injected into the tumor, whereas it was applied into the resection cavity in the remaining 14 cases. Neoadjuvant application of radiolabeled DOTAGA-SP as first-line treatment before resection has been done in two low-grade gliomas (cases 19 and 20), which was well tolerated. Eight primary or secondary lesions had been resected following i.t. injection of radiolabeled DOTAGA-SP, histologically showing extensive radiation necrosis. Surgery was found to be considerably facilitated (Supplementary Video) because of a better demarcation of tumor margins and a reduction of intraoperative bleeding as a result of radiation effects on the tumor vasculature (23). The maximum range of ^{90}Y is only 12 mm. This means that radiation alone without a process of biodistribution cannot explain the histologic finding of radiation necrosis. This finding at the tumor periphery several centimeters distant from the site of injection suggests a rapid process of diffusion of the low molecular weight compound DOTAGA-SP to mainly contribute to local biodistribution of the radiopharmaceutical, which may also be supported by a slower process of convection.

Late radiation necrosis with mass effect and functional deterioration has frequently been observed following interstitial radiotherapy using ^{125}I seeds (45). In the neoadjuvant approach (i.e., targeted β-radiotherapy) followed by surgical debulking, induction of extensive radiation necrosis represents one of the goals of treatment. If a glioma is not resectable due to critical location, low-range β- and/or α-emitters should be used to minimize collateral neurologic damage, as done for cases 1, 4, 15, 16, and 18. ^{177}Lu and ^{213}Bi have a maximum range of 1.5 and 0.06 mm, respectively, compared with 12 mm of ^{90}Y. Therapeutic α-protocols may be best suited for invasive tumor cells beyond visible tumor margins. We always conducted secondary resection of irradiated large and accessible tumors. During the observational phase, interpretation of a new enhancing ring-like structure can be difficult, especially in

low-grade gliomas. In these cases, perfusion CT was found to be useful to differentiate hypovascular radionecrosis from vital neoplastic tissue (Fig. 3D and E). *De novo* ring-like calcification indicates radiation necrosis (Fig. 3C and F), which was histologically proven by lesion resection 26 months after DOTAGA-SP treatment (Supplementary Video). As mentioned above, surgery was significantly facilitated by pretreating the lesion with this targeted approach, which created a sharply demarcated calcified lesion with reactive glial reaction. Normally, identification of tumor boarders when resecting a not-pretreated low-grade glioma is virtually impossible.

In conclusion, targeted radiotherapy using the radiolabeled diffusible peptidic vector DOTAGA-SP represents an innovative strategy for local control of malignant gliomas of WHO grades 2 to 4, which will be further examined for i.t. and intracavitary injections in future clinical trials.

Acknowledgments

We thank the medical and technical staff of the Neurosurgical and Nuclear Medicine Clinics and the technical staff of the Division of Radiological Chemistry in supporting this study.

References

1. Kleihues P, Burger P, Scheithauer B. Histological typing of tumours of the central nervous system. WHO, international histological classification of tumours. 2nd ed. Berlin (Germany): Springer; 1993.
2. Maher EA, Furnari FB, Bachoo RM, et al. Malignant glioma: genetics and biology of a grave matter. Genes Dev 2001;15:1311–33.
3. Merlo A. Genes and pathways driving glioblastomas in humans and murine disease models. Neurosurg Rev 2003;26:145–58.
4. Shaw EG, Scheithauer BW, O'Fallon JR, Tazelaar HD, Davis DH. Oligodendrogliomas: the Mayo Clinic experience. J Neurosurg 1992;76:428–34.
5. Stupp R, Mason WP, van den Bent MJ, et al. Radiotherapy plus concomitant and adjuvant temozolomide for glioblastoma. N Engl J Med 2005;352:987–96.
6. Walker MD, Green SB, Byar DP, et al. Randomized comparisons of radiotherapy and nitrosoureas for the treatment of malignant glioma after surgery. N Engl J Med 1980;303:1323–9.
7. Hegi ME, Diserens AC, Gorlia T, et al. MGMT gene silencing and benefit from temozolomide in glioblastoma. N Engl J Med 2005;352:997–1003.
8. Oertel J, von Buttlar E, Schroeder HW, Gaab MR. Prognosis of gliomas in the 1970s and today. Neurosurg Focus 2005;18:e12.
9. Burger PC. What is an oligodendroglioma? Brain Pathol 2002;12:257–9.
10. Keene DL, Hsu E, Ventureyra E. Brain tumors in childhood and adolescence. Pediatr Neurol 1999;20:198–203.
11. Hochberg FH, Pruitt A. Assumptions in the radiotherapy of glioblastoma. Neurology 1980;30:907–11.
12. Laske DW, Youle RJ, Oldfield EH. Tumor regression with regional distribution of the targeted toxin TF-CRM107 in patients with malignant brain tumors. Nat Med 1997;3:1362–8.
13. Kawakami K, Kawakami M, Kioi M, Husain SR, Puri RK. Distribution kinetics of targeted cytotoxin in glioma by bolus or convection-enhanced delivery in a murine model. J Neurosurg 2004;101:1004–11.
14. Rand RW, Kreitman RJ, Patronas N, Varricchio F, Pastan I, Puri RK. Intratumoral administration of recombinant circularly permuted interleukin-4-*Pseudomonas* exotoxin in patients with high-grade glioma. Clin Cancer Res 2000;6:2157–65.
15. Cokgor I, Akabani G, Kuan CT, et al. Phase I trial results of iodine-131-labeled antitenascin monoclonal antibody 81C6 treatment of patients with newly diagnosed malignant gliomas. J Clin Oncol 2000;18:3862–72.
16. Merlo A, Jermann E, Hausmann O, et al. Biodistribution of ^{111}In-labelled SCN-bz-DTPA-BC-2 MAb following loco-regional injection into glioblastomas. Int J Cancer 1997;71:810–6.
17. Riva P, Arista A, Franceschi G, et al. Local treatment of malignant gliomas by direct infusion of specific monoclonal antibodies labeled with ^{131}I: comparison of the results obtained in recurrent and newly diagnosed tumors. Cancer Res 1995;55:5952–6s.
18. Maecke HR. Radiolabeled peptides in nuclear oncology: influence of peptide structure and labeling strategy on pharmacology. Ernst Schering Res Found Workshop 2005:43–72.
19. Otte A, Mueller-Brand J, Dellas S, Nitzsche EU, Herrmann R, Maecke HR. Yttrium-90-labelled somatostatin-analogue for cancer treatment. Lancet 1998;351:417–8.
20. Waldherr C, Pless M, Maecke HR, Haldemann A, Mueller-Brand J. The clinical value of [^{90}Y-DOTA]-D-Phe^1–Tyr^3-octreotide (^{90}Y-DOTATOC) in the treatment of neuroendocrine tumours: a clinical phase II study. Ann Oncol 2001;12:941–5.
21. Beutler D, Avoledo P, Reubi JC, et al. Three-year recurrence-free survival in a patient with recurrent medulloblastoma after resection, high-dose chemotherapy, and intrathecal Yttrium-90-labeled DOTA^0-D-Phe^1-Tyr^3-octreotide radiopeptide brachytherapy. Cancer 2005;103:869–73.
22. Merlo A, Hausmann O, Wasner M, et al. Locoregional regulatory peptide receptor targeting with the diffusible somatostatin analogue ^{90}Y-labeled DOTA^0-D-Phe^1-Tyr^3-octreotide (DOTATOC): a pilot study in human gliomas. Clin Cancer Res 1999;5:1025–33.
23. Hennig IM, Laissue JA, Horisberger U, Reubi JC. Substance-P receptors in human primary neoplasms: tumoral and vascular localization. Int J Cancer 1995;61:786–92.
24. Beaujouan JC, Torrens Y, Saffroy M, Kemel ML, Glowinski J. A 25 year adventure in the field of tachykinins. Peptides 2004;25:339–57.
25. Mitrovic B, Martin FC, Charles AC, et al. Neurotransmitters and cytokines in CNS pathology. Prog Brain Res 1994;103:319–30.
26. Furnari FB, Lin H, Huang HS, Cavenee WK. Growth suppression of glioma cells by PTEN requires a functional phosphatase catalytic domain. Proc Natl Acad Sci U S A 1997;94:12479–84.
27. Ishii N, Maier D, Merlo A, et al. Frequent co-alterations of TP53, p16/CDKN2A, p14^{ARF}, PTEN tumor suppressor genes in human glioma cell lines. Brain Pathol 1999;9:469–79.
28. Maier D, Jones G, Li X, et al. The PTEN lipid phosphatase domain is not required to inhibit invasion of glioma cells. Cancer Res 1999;59:5479–82.
29. Schmassmann A, Waser B, Flogerzi B, Reubi JC. Expression of functional neurokinin-1 receptors in regenerative glands during gastric wound healing in rodents. Gastroenterology 2004;126:784–95.
30. Reubi JC, Waser B, Schaer JC, Laissue JA. Somatostatin receptor sst1-5 expression in normal and neoplastic human tissues using receptor autoradiography with subtype-selective ligands. Eur J Nucl Med 2001;28:836–46.
31. Atherton E, Sheppard R. Fluorenylmethoxycarbonyl-polyamide solid phase peptide synthesis. General principles and development. Oxford: Information Press Oxford; 1989.
32. Eisenwiener KP, Powell P, Maecke HR. A convenient synthesis of novel bifunctional prochelators for coupling to bioactive peptides for radiometal labelling. Bioorg Med Chem Lett 2000;10:2133–5.
33. Apostolidis C, Carlos-Marquez R, Janssens W, Molinet R, Nikula T, Ouadi A. Cancer treatment using ^{213}Bi and ^{225}Ac in radioimmu-notherapy. Nuclear News 2001;44:29–33.
34. Macdonald DR, Cascino TL, Schold SC, Jr., Cairncross JG. Response criteria for phase II studies of supratentorial malignant glioma. J Clin Oncol 1990;8:1277–80.
35. Schumacher T, Hofer S, Eichhorn K, et al. Local injection of the ^{90}Y-labelled peptidic vector DOTATOC to control gliomas of WHO grades II and III: an extended pilot study. Eur J Nucl Med Mol Imaging 2002;29:486–93.
36. Ruser G, Ritter W, Maecke HR. Synthesis and evaluation of two new bifunctional carboxymethylated tetraazamacrocyclic chelating agents for protein labeling with indium-111. Bioconjug Chem 1990;1:345–9.
37. Sangha H, Lipson D, Foley N, et al. A comparison of the Barthel index and the functional independence measure as outcome measures in stroke rehabilitation: patterns of disability scale usage in clinical trials. Int J Rehabil Res 2005;28:135–9.
38. Cervera P, Videau C, Viollet C, et al. Comparison of somatostatin receptor expression in human gliomas and medulloblastomas. J Neuroendocrinol 2002;14:458–71.
39. Reubi JC, Lang W, Maurer R, Koper JW, Lamberts SW. Distribution and biochemical characterization of somatostatin receptors in tumors of the human central nervous system. Cancer Res 1987;47:5758–64.
40. Good S, Maecke HR. Stability and kinetics of formation of two macrocyclic chelator-conjugtes with ^{177}Lu. Nuklearmedizin 2004;43:A11.
41. Moll S, Nickeleit V, Mueller-Brand J, Brunner FP, Maecke HR, Mihatsch MJ. A new cause of renal thrombotic microangiopathy: yttrium 90-DOTATOC internal radiotherapy. Am J Kidney Dis 2001;37:847–51.
42. Carson BS, Sr., Wu Q, Tyler B, et al. New approach to tumor therapy for inoperable areas of the brain: chronic intraparenchymal drug delivery. J Neurooncol 2002;60:151–8.
43. Reardon DA, Akabani G, Coleman RE, et al. Phase II trial of murine ^{131}I-labeled antitenascin monoclonal antibody 81C6 administered into surgically created resection cavities of patients with newly diagnosed malignant gliomas. J Clin Oncol 2002;20:1389–97.
44. Parney IF, Kunwar S, McDermott M, et al. Neuroradiographic changes following convection-enhanced delivery of the recombinant cytotoxin interleukin 13-PE38QQR for recurrent malignant glioma. J Neurosurg 2005;102:267–75.
45. Wowra B, Schmitt HP, Sturm V. Incidence of late radiation necrosis with transient mass effect after interstitial low dose rate radiotherapy for cerebral gliomas. Acta Neurochir (Wien) 1989;99:104–8.
46. Reubi JC, Horisberger U, Lang W, Koper JW, Braakman R, Lamberts SW. Coincidence of EGF receptors and somatostatin receptors in meningiomas but inverse, differentiation-dependent relationship in glial tumors. Am J Pathol 1989;134:337–44.